Electromagnetic backgrounds in neutrino-produced trimuon events

J. Smith
Institute for Theoretical Physics, State University of New York at Stony Brook, Stony Brook, New York 11794

J. A. M. Vermaseren
Department of Physics, Purdue University, West Lafayette, Indiana 47907

(Received 28 November 1977)

We discuss the electromagnetic production of $\mu^+\mu^-$ pairs in neutrino-induced reactions. The cross section for $\nu_\mu + N \to \mu^- + \mu^- + \mu^+ + X$ is calculated, using a quark-parton model for the photon-hadron interaction, and is $\sim 0.3 \times 10^{-4}$ of the normal inclusive cross section for $\nu_\mu + N \to \mu^- + X$. The precise value depends upon the neutrino spectrum and experimental cuts. We present several distributions which exhibit characteristic features expected from this electromagnetic process. Corresponding reactions involving e^+e^- pairs are also studied because such events should be seen rather easily in bubble-chamber experiments. We also give some results for antineutrino-induced interactions leading to $\mu^+\mu^+\mu^-$ events.

I. INTRODUCTION

Recently trimuon events have been discovered by the Caltech-Fermilab[1] (CF), Fermilab-Harvard-Pennsylvania-Rutgers-Wisconsin[2] (FHPRW), and CERN-Dortmund-Heidelberg-Saclay[3] (CDHS) groups in neutrino and antineutrino experiments at Fermilab and CERN. The source of these events is still unclear, but the high rate reported initially by the FHPRW group[2] led to considerable speculation that such events were due to the production and decay of new heavy leptons or heavy quarks either produced singly or in association.[4] Detailed phenomenological studies have been made to distinguish between these mechanisms. An alternative model, namely diffractive dissociation,[5] has also been proposed as an explanation of these events.

In this paper we consider a different mechanism which can generate trimuon events in neutrino and antineutrino beams, namely the radiative processes creating muon Dalitz pairs, viz.,

$$\nu_\mu(\bar{\nu}_\mu) + N \to \mu^-(\mu^+) + \text{“}\gamma\text{”} + X \qquad (1)$$
$$\text{“}\gamma\text{”} \to \mu^+ + \mu^-,$$

where “γ” is a virtual photon. The electromagnetic production of real vector mesons is discussed in a paper by Godbole.[6] The process we investigate, depicted in Fig. 1, is a hard-photon reaction similar to single-photon bremsstrahlung graphs in e^+e^- collisions. The key signature for such a process is a severe peaking of one dimuon invariant-mass distribution for small masses which reflects the infrared-divergent nature of quantum-electrodynamic processes.

Clearly a model must be used to calculate the graphs in Fig. 1. In the ν interaction a negatively charged muon is produced in association with a positively charged W boson. The positive charge is then communicated to the hadron shower through the production of quarks which become real hadrons. Whether the quarks radiate the photon or the hadrons radiate the photon is unclear. The most obvious model is one where the quarks radiate the photon so that the basic set of Feynman diagrams is those shown in Fig. 2. However, it would be very interesting to check that this is indeed the case by studying the analogous reaction with a muon beam, i.e., the production of muon tridents. The classic experiment in this field by Russell *et al.*[7] measured tridents for the first time and conclusively showed that muons obey Fermi-Dirac statistics. A low-energy muon beam was used, so the assumptions behind the quark-parton model were not tested. In the recent experiment by Chang *et al.*[8] at Fermilab, 11 trimuon events were reported with a rate larger than expected from normal QED-type processes. The excess can be explained by the associated production

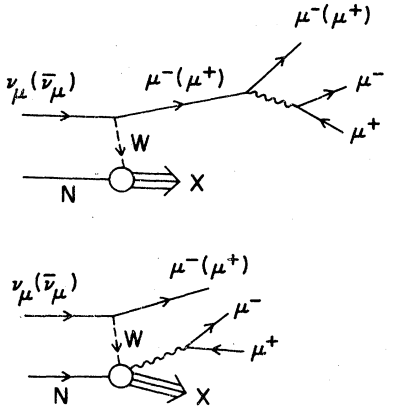

FIG. 1. Feynman diagrams for the reaction $\nu_\mu(\bar{\nu}_\mu) + N \to \mu^-(\mu^+) + \mu^+ + \mu^- + X$.

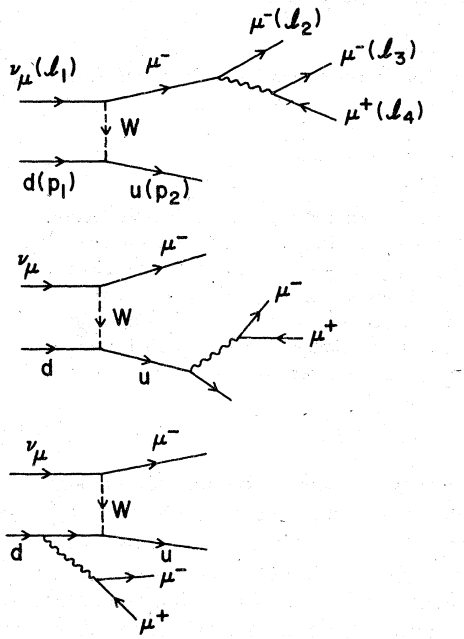

FIG. 2. Feynman diagrams for the reaction $\nu_\mu + d \to d \to \mu^- + \mu^+ + \mu^- + \mu$.

of charmed particles[9] which subsequently undergo semileptonic decay modes. In a SLAC experiment, Fancher *et al.*[10] have measured the e^+e^- asymmetry in deep-inelastic bremsstrahlung and found it to be consistent with the quark-parton model, although they were unable to distinguish between fractionally charged and integrally charged quarks. The final photon in this experiment was on the mass shell as contrasted to our case where the photon has a timelike mass. Finally, we should mention that earlier experiments on the photoproduction of muon pairs[11] and inelastic Compton scattering[12] do not test our assumptions because they used real photon beams so the underlying physics is different. Each of these experiments reported an excess of events when their rates were compared to quark-parton-model calculations. None of the experiments listed above are conclusive in proving that quark-parton-model ideas can be applied to the muon trident situation in the kinematic region we require. However, even without this check, it is reasonable to assume that the radiation of low-mass muon pairs can be reliably calculated using such an approach.

Thus we base the analysis in this paper on a quark-parton radiation model. Although qualitative estimates for the rate for such reactions can be written down rather easily, quantitative calculations are necessary to obtain a detailed understanding of the process. From an experimental point of view this reaction is uninteresting and constitutes a background which must be removed from the data sample before other more exotic mechanisms can be investigated. The radiation from the charged muon involves no new physics, so, from a theoretical point of view, the reaction may be of interest if we can learn something about photon quark couplings. Note that the soft-photon radiative corrections to neutrino interactions have been calculated by Kiskis.[13]

In Sec. II we first made a rather simple estimate of the trimuon event rate by considering the total cross section for the reaction $\nu_\mu + d \to \mu^- + \mu^- + \mu^+ + u$ on pointlike up and down quarks with mass equal to that of the proton. This cross section is interesting because it can be compared with the corresponding cross section for $\nu_\mu + d \to \mu^- + u$ to estimate the trimuon production rate. At this stage it is also interesting to give results for the antineutrino-induced reaction $\bar{\nu}_\mu + u \to \mu^+ + \mu^- + \mu^+ + d$ and compare it to the usual reaction $\bar{\nu}_\mu + u \to \mu^+ + d$. Both the radiative and nonradiative antineutrino cross sections are a factor of 3 smaller than their corresponding neutrino counterparts. By switching the μ^+ and μ^- masses to those of an electron, we can also give results for the total cross sections for producing an electron-positron pair in neutrino and antineutrino interactions. All these cross sections are upper bounds for the reactions because the inclusion of the quark-parton distribution function $F_2(x)$ reduces the cross sections. Our approximation of

$$R = \sigma(\nu_\mu + N \to \mu^- + \mu^- + \mu^+ + X)/\sigma(\nu_\mu + N \to \mu^- + X)$$

by

$$R' = \sigma(\nu_\mu + d \to \mu^- + \mu^- + \mu^+ + u)/\sigma(\nu_\mu + d \to \mu^- + u)$$

is by no means a rigorous calculation of the true event rate, but serves to give an idea of its magnitude.

In the second part of Sec. II we therefore proceed to examine a more realistic model, which includes quark-parton distribution functions, to calculate the event rate R for an isoscalar target. The quadrupole-triplet spectrum is included and appropriate experimental cuts are made on the energies and angles of the detected muons. We also add a cut that $E_\nu \equiv E_{\rm vis}$ must be larger than 100 GeV and find that $R = 0.28 \times 10^{-4}$. Note that there is no missing energy in this electrodynamic process in contrast to the other models proposed to explain the trimuon events[4] which involve the production and decay of new particles and therefore have missing neutrinos. As a further refinement, we also consider the effect of the Pauli exclusion principle by adding the set of graphs with the two negative muons interchanged. We close this section with some comments on the event rates for

the radiative processes involving both $\mu^+\mu^-$ and e^+e^- pairs, assuming that they are produced in the quadrupole-triplet neutrino spectrum.

In Sec. III we present several distributions which are characteristic of the electrodynamic production of muon and electron pairs. Our objective is to find the best cuts to isolate this background, so that it can be studied in more detail, or subtracted to see if other trimuon production mechanisms are present. We note in particular the severe peaking of the dilepton invariant-mass distribution involving the slow μ^- and the μ^+. Future experiments with larger data samples will see this process rather easily. We also examine the probability that the two extremely energetic events reported by the FHPRW group can be accounted for by electromagnetic processes.

For completeness we comment on results for the antineutrino production of $\mu^+\mu^+\mu^-$ events. We also discuss the production of e^+e^- pairs. The rate for the latter reaction is reasonably large, but there will be a severe background due to π^0 Dalitz decays so only events with e^+e^- invariant masses larger than the pion mass can be used as a signal. Finally, in Sec. IV we give our conclusions.

II. CALCULATIONS

We now proceed to investigate the diagrams depicted in Fig. 1, using the quark-parton model. We refrain from calling this process trident production because the term usually refers to a Bethe-Heitler–type reaction where the neutrino (muon) dissociates into other leptons in the Coulomb field of a nucleus.[14] Muon-Dalitz-pair production is a better name for reaction (1) because the virtual photon is in the timelike region. Our basic assumption is that the proton (isoscalar target) is made up of quarks and the photon interacts with them in a pointlike fashion. In this simple model one only needs to calculate the cross section for the graphs shown in Fig. 2. Then, by dividing by the cross section for the nonradiative process, also calculated for free quarks, the event rate for trimuons can be estimated. If we subsequently incorporate the neutrino flux and the experimental cuts, we can give an answer for the trimuon event rate. The FHPRW group quotes an uncorrected rate for

$$R=\sigma(\nu_\mu+N\to\mu^-+\mu^-+\mu^++X)/\sigma(\nu_\mu+N\to\mu^-+X)$$
$$=5\times10^{-4}$$

for $E_\nu>100$ GeV, using the quadrupole-triplet neutrino spectrum, and imposing cuts such that for each muon $E_\mu>4$ GeV and $\theta_\mu\lesssim400$ mr. We will use the same cuts. Clearly if our crude calculation for R yields answers which are far too small, then there is no need to worry about electromagnetic backgrounds at the present time. However, if our answer turns out to be close to the experimental number, then a more refined calculation is necessary. We find the latter situation to be indeed the case and therefore present a more elaborate calculation in the second part of this section.

A. Simple model

We assume that the dominant quantum-electrodynamical process giving rise to muon Dalitz pairs is radiation from the muon and quark lines. Thus we calculate the cross section for

$$\nu_\mu(l_1)+d(p_1)\to\mu^-(l_2)+\mu^-(l_3)+\mu^+(l_4)+u(p_2),$$

where u and d refer to the usual up and down quarks. If we adopt the same simple picture for the basic reaction $\nu_\mu+d\to\mu^-+u$, then we can use ratios of cross sections for

$$\sigma(\nu_\mu+d\to\mu^-+\mu^-+\mu^++u)/\sigma(\nu_\mu+d\to\mu^-+u)$$

to estimate the real event rate, i.e.,

$$\sigma(\nu_\mu+N\to\mu^-+\mu^-+\mu^++X)/\sigma(\nu_\mu+N\to\mu^-+X),$$

where N represents an isoscalar target. The cross section for $\nu_\mu+d\to\mu^-+u$ rises linearly with the beam energy, whereas we expect the cross section for the radiative process $\nu_\mu+d\to\mu^-+\mu^-+\mu^++u$ to have additional logarithms in the beam energy. We can estimate the dependence on E_ν by fitting the results from our computer programs so we have not derived an asymptotic expansion of the cross section for large beam energy.

Therefore, in this simple model, we ignore the Pauli exclusion principle and leave out the corresponding set of graphs with $\mu^-(l_2)$ and $\mu^-(l_3)$ interchanged. Also, we do not initially take the structure functions of the nucleon or isoscalar target into account. These effects will clearly have some influence on our results, because the exclusion principle tends to depopulate the region of phase space where the two negative muons have identical energies and angles, and the structure functions induce a weighting in the x variable. We include these additional effects in the second part of this section. In a first approximation inclusion of structure functions tends to affect both the numerator and denominator of R' in the same way.

Using the above notation, the matrix element for the diagrams in Fig. 2 is given by

$$\mathfrak{M}=\frac{e^2G_F}{\sqrt{2}}\frac{1}{k^2}\bar{u}(l_3)\gamma_\alpha v(l_2)\left[\bar{u}(l_2)\frac{2l_{2\alpha}+\gamma_\alpha \not{k}}{2k\cdot l_2+k^2}\gamma_\mu(1+\gamma_5)u(l_1)\bar{u}(p_2)\gamma_\mu(1-\gamma_5)u(p_1)\right.$$
$$-\tfrac{2}{3}\bar{u}(l_2)\gamma_\mu(1+\gamma_5)u(l_1)\bar{u}(p_2)\frac{2p_{2\alpha}+\gamma_\alpha \not{k}}{2k\cdot p_2+k^2}\gamma_\mu(1-\gamma_5)u(p_1)$$
$$\left.-\tfrac{1}{3}\bar{u}(l_2)\gamma_\mu(1+\gamma_5)u(l_1)\bar{u}(p_2)\gamma_\mu(1-\gamma_5)\frac{2p_{1\alpha}-\not{k}\gamma_\alpha}{2k\cdot p_1-k^2}u(p_1)\right], \tag{2}$$

where k is the four-momentum of the virtual photon. We used the program SCHOONSCHIP[15] to complete the square of the matrix element. We did not make any attempt to rearrange terms because we have computer programs which can easily handle cancellations between the graphs and at the same time the potentially infrared-divergent dependence on the mass of the virtual photon. The expression for the cross section is

$$\sigma=\frac{1}{2(s-M^2)}\frac{1}{(2\pi)^8}\int\frac{d^3l_2}{2E_2}\int\frac{d^3l_3}{2E_3}\int\frac{d^3l_4}{2E_4}\int\frac{d^3p_2}{2\omega_2}\delta(l_1+p_1-l_2-l_3-l_4-p_2)\tfrac{1}{2}|\mathfrak{M}|^2,$$

where the factor of $\frac{1}{2}$ arises from the spin average and M is the mass of the d quark. We now introduce the timelike variable $k^2=(l_3+l_4)^2$ by addition of a δ function in the usual way, thereby splitting the integrations into two blocks. The first block contains the usual two-to-three-body kinematics while the second block contains the decay of the virtual photon. Hence we get

$$\sigma=\frac{1}{2(s-M^2)}\frac{1}{(2\pi)^8}\int\frac{d^3l_2}{2E_2}\int\frac{d^3p_2}{2\omega_2}\int\frac{d^3k}{2E_k}\delta(l_1+p_1-l_2-k-p_2)\int dk^2\int\frac{d^3l_3}{2E_3}\int\frac{d^3l_4}{2E_4}\delta(k-l_3-l_4)\tfrac{1}{2}|\mathfrak{M}|^2. \tag{3}$$

Evaluating the l_3 and l_4 integrations in the rest frame of k we get the final expression

$$\sigma=\frac{\alpha^2G_F{}^2}{64\pi^5(s-M^2)}\left\{\frac{\pi}{16(s-M^2)}\int\frac{ds_1dt_1ds_2dt_2}{[-\Delta(l_1,l_2,p_1,p_2)]^{1/2}}\right\}\int dk^2\left(1-\frac{4m^2}{k^2}\right)^{1/2}\int\frac{d\Omega}{4\pi}\left(\frac{1}{k^4}|\mathfrak{M}'|^2\right), \tag{4}$$

where s_1, s_2, t_1, and t_2 are the usual multiperipheral variables for two-to-three-body reactions, m is the muon mass, Δ is the Gram determinant, and $\mathfrak{M}'$ is defined by the relation $|\mathfrak{M}|^2=2e^4G_F{}^2\times|\mathfrak{M}'|^2/k^4$. The integrations were handled numerically using mappings to smooth out the distributions. We give the total cross section in Fig. 3 for the case where the quark mass is taken to be the nucleon mass. Clearly the value for this cross section is reasonably large. A rough numerical fit to this curve for $E_\nu\gtrsim 25$ GeV gives the cross section (E_ν is in GeV units)

$$\sigma(\nu_\mu+d\to\mu^-+\mu^-+\mu^++X)$$
$$=1.0\times E_\nu\ln\left(\frac{E_\nu}{14}\right)\times10^{-42}\ \text{cm}^2, \tag{5}$$

demonstrating the additional logarithmic dependence on the beam energy.

The corresponding reaction $\bar{\nu}_\mu+u\to\mu^++\mu^-+\mu^++d$ can also be calculated using either convenient substitutions or by squaring the new matrix element. We expect this cross section to be reduced by approximately a factor of 3, analogous to the case of $\sigma(\bar{\nu}_\mu+u\to\mu^++d)$ versus $\sigma(\nu_\mu+d\to\mu^-+u)$. The result is also shown in Fig. 3 and answers our expectations. Finally we evaluate the cross sections for the reactions $\nu_\mu+d\to\mu^-+e^++e^-+u$ and $\bar{\nu}_\mu+u\to\mu^++e^++e^-+d$ and add them to Fig. 3 also. The latter cross sections are larger than we originally expected. In fact, it would be interesting to derive an asymptotic expansion for the cross section to find its explicit dependence on the particle masses. Clearly these cross sections can all be fitted by expressions of the type shown in Eq. (5). Our computer results for the seven-dimensional integral are not accurate enough to distinguish between a formula containing two powers of a logarithm and a formula containing one power. Typically the accuracy on the muon cross sections is of the order of 5% and on the electron cross sections of the order of 15%. The errors can easily be made smaller, but there is no need for such accuracy at the present time. In evaluating these results we only used 15 000 points in the integration region.

We are now ready to give some approximate answers for the $\mu^-\mu^-\mu^+$ event rate in a neutrino beam. The regular formula for the charged-current reaction on pointlike quarks is

$$\sigma(\nu_\mu+d\to\mu^-+u)=\frac{G_F{}^2 2ME}{\pi}$$
$$=3.1\times(E_\nu\ \text{in GeV})\times10^{-38}\ \text{cm}^2, \tag{6}$$

so the ratio of the cross sections, which cancels the linear dependence upon the quark mass, yields

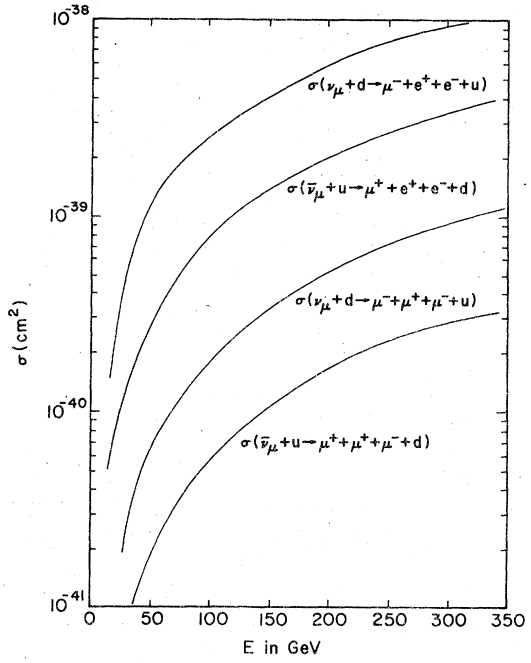

FIG. 3. Total cross sections for the reactions $\nu_\mu + d \to \mu^- + \mu^+ + \mu^- + u$, $\nu_\mu + d \to \mu^- + e^+ + e^- + u$, $\bar{\nu}_\mu + u \to \mu^+ + \mu^+ + \mu^- + d$, and $\bar{\nu}_\mu + u \to \mu^+ + e^+ + e^- + d$.

the answer

$$R' = 0.3 \times \ln\left(\frac{E_\nu}{14}\right) \times 10^{-4}. \tag{7}$$

For 100-GeV neutrinos we therefore find

$$R' = 0.6 \times 10^{-4}. \tag{8}$$

This number is uncomfortably close to the experimental value reported by the FHPRW group. If we also compare this rate with the value reported by the CDHS group namely, $R = 0.8 \times 10^{-4}$, if $E_\nu > 100$ GeV and 0.4×10^{-4} for all E_ν, then it is clear that the electromagnetic background process cannot be ignored. Hence we have to make a more refined calculation. To get a feeling for the inclusion of additional effects we take our previous result, add the quadrupole-triplet spectrum, make cuts on the muon energies and angles, and finally add the restriction that $E_\nu > 100$ GeV. With these additions, the normalized flux-averaged expression becomes 1.3×10^{-40} cm^2 over the full range of E_ν and 2.0×10^{-40} for $E_\nu > 100$ GeV. The reason our answer increases is due to the smaller flux of neutrinos above 100 GeV. If we repeat the same analysis for the regular cross section, then the flux-averaged expression in Eq. (6), i.e., 2.26×10^{-36} for all E_ν, is changed into 5.07×10^{-36} for $E_\nu > 100$ GeV, again the increase reflecting the smaller flux of neutrinos above 100 GeV. Taking the ratio of the numbers we therefore find

$$R' = \left.\frac{\sigma(\nu_\mu + d \to \mu^- + \mu^- + \mu^+ + u)}{\sigma(\nu_\mu + d \to \mu^- + u)}\right|_{E_\nu > 100\ \mathrm{GeV}}$$

$$= 0.4 \times 10^{-4}. \tag{9}$$

There is therefore a small reduction due primarily to the fact that the energy and angle cuts on the muons decrease the numerator more than the denominator.

Note that the event rate for the production of $\mu^+\mu^+\mu^-$ events in an antineutrino beam has almost the same value as given by Eq. (8) because the factor of one third is common to both the radiative and nonradiative reactions. The other numbers, i.e., in Eq. (9), only hold after flux-averaging so they are not exactly applicable to antineutrino beams. However, using the fact that the antineutrino spectra generally peak at the same energy as the neutrino spectra and the cross sections have the same dependence on beam energy, we can use the above results to a good approximation for antineutrinos. In any comparison of neutrino and antineutrino rates then the different spectra will have to be taken into account. Also, for the same reason the numbers we give for electron rates are not immediately useful for bubble-chamber physicists. In that case, different spectra and cuts are used which have to be incorporated into our programs. The qualitative features we describe here using the quadrupole-triplet spectrum continue to hold in other situations, although quantitative results may change.

The radiative cross sections as calculated above depend linearly upon the mass of the quark as do the cross sections for the nonradiative processes. By taking the ratio we have canceled this common factor so that our answers now depend logarithmically on the quark mass. The principal justification for presenting the result in Eq. (5) is that it represents an upper bound for the radiative cross section from valence quarks. Including distribution functions for the quarks means adding an additional probability distribution $F_2(x)$ which is smaller than unity and therefore reduces the cross section. Also note that we have calculated the radiation from valence quarks only. Radiation from sea quarks (and maybe gluons) will tend to increase the value of the basic cross section, but within the framework of our model these are assumed to be small effects. We now proceed to discuss a more reasonable model for the reaction.

B. Realistic model

We now refine our simple model by the addition of quark-parton distribution functions and the effects due to the Pauli exclusion principle. The former effect is the more important of the two.

However, it is unjustified to drop the latter, which tends to depress the distribution in the invariant mass of the pair and consequently lowers the value of the radiative cross section.

The inclusion of distribution functions for the quarks can be handled in a straightforward fashion. Instead of keeping the final-quark mass on-shell, this variable should now be integrated over the allowed range for the inclusive production. Usually one transforms the integration over the variables q^2 and W^2 to an integration over the variables x and y and multiplies by the appropriate distribution function for the quarks. The easiest way for us to implement the effect of the distribution function is by analogy with the corresponding case for the regular inclusive cross section. In that case we scale the variable $s \to xs$ and average over the sum of the distribution functions for up and down quarks. Hence, for an *isoscalar* target

$$\sigma(\nu_\mu + N \to \mu^- + X) = \frac{G^2}{\pi} M_N E_\nu \int F_2(x) dx \,, \tag{10}$$

where

$$F_2(x) = x[u(x) + d(x)]_{\text{val}} + x[u(x) + d(x)]_{\text{sea}} \,,$$

with[16]

$$\begin{aligned} x[u(x) + d(x)]_{\text{val}} &= 1.74\sqrt{x}\,(1-x)^3(1+2.3x) \\ &\quad + 1.11\sqrt{x}\,(1-x)^{3.1} \,, \\ x[u(x) + d(x)]_{\text{sea}} &= 0.2(1-x)^{3.5} \,, \end{aligned} \tag{11}$$

and M_N the mass of the nucleon.[17] Calculating the integral over x and adding the flux average yields answers for Eq. (10) of 0.52×10^{-36} for all E_ν and 1.15×10^{-36} for $E_\nu > 100$ GeV.

For the radiative reaction we should actually transform the square of our matrix element into the infinite-momentum frame where the mass of the quark is negligible. From a practical point of view, almost all of the dependence on the quark mass can be eliminated by transforming the square of the matrix element to a fast-moving frame, which, for simplicity, we chose as the neutrino nucleon center-of-mass frame. In this frame the target quark has an energy of $(s + M^2)/2\sqrt{s} \simeq 10$ GeV for $E_\nu \simeq 100$ GeV so the effect of retaining a small quark mass is negligible. We then scale the quark center-of-mass three-momentum and weight the square of the matrix element by the distribution function $F_2(x)$. No attempt is made to include the transverse momentum of the quark. Since, for any configuration, the cross section only depends on $s' = (l_1 + p_1)^2$ we can evaluate it in any frame, and therefore choose the laboratory frame. The result of these manipulations is that the scale of the cross section is now set by the nucleon mass, just as in Eq. (10), and therefore our answers are essentially independent of the mass of the quark. The neutrino scattering is actually from an isoscalar target, so we have to include both the contributions from the d quark in the proton and the d quark in the neutron. However, the contribution from the d quark in the neutron is essentially the same as that of the u quark in the proton so we are justified in adding the two contributions (analogous to the nonradiative process). We therefore take the same distribution functions as given in Eq. (11) for the radiative process. The inclusion of a small amount of sea quarks does not produce large changes in our results. If we now evaluate the cross section and fold it with the quadrupole-triplet neutrino spectrum, then we find $\sigma(\nu_\mu + N \to \mu^- + \mu^- + \mu^+ + X) = 0.15 \times 10^{-40}$ for E_ν and $= 1.33 \times 10^{-40}$ for $E_\nu > 100$ GeV with all the other cuts. Division by the regular cross sections given above then yields $R = 0.29 \times 10^{-4}$ for all E_ν and $R = 0.28 \times 10^{-4}$ for $E_\nu > 100$ GeV and all muon cuts. The reduction in R due to the inclusion of the quark-parton distribution function changes some of the final distributions, but not so severely as one might expect. We have studied the dependence of these numbers on the quark mass over the range 5 to 300 MeV and found it to be very small.

A corresponding reduction holds for antineutrinos producing $\mu^+\mu^+\mu^-$ events and for neutrino/antineutrino production of $\mu^-e^+e^-$ and $\mu^+e^+e^-$ events, respectively. Modulo our comments regarding the spectra one can estimate these event rates from the numbers given above.

The Pauli exclusion principle should also be included in this calculation for completeness. This effect reduces the cross section for the production of muon tridents and was studied by Russell *et al.*[7] in an experiment at BNL. When the invariant-mass distribution of the two like-sign muons was measured, it was found to be in good agreement with theoretical expectations. Note that the magnitude of the effect was approximately 30% at a beam energy of 10.5 GeV, using an iron target. We expect to see similar changes in our cross-section values because all the muon energy distributions peak at low energies. The Pauli exclusion principle has not been included in other studies of trimuon production[4,5] because the muons generally arose from the decays of different particles but, in principle, it should have been included. In our case, the probability of producing two μ^- particles with the same energy and angle is not negligible, and the additional work to include the Pauli-principle effect is rather small, so there is no need to neglect it. To our knowledge, this is the first time this effect has been included in a reaction where both the weak and electromagnetic interactions play an important role.

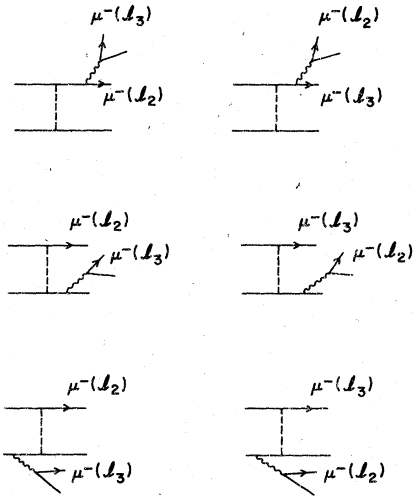

FIG. 4. Feynman diagrams for the reaction $\nu_\mu + d \rightarrow \mu^- + \mu^+ + \mu^- + u$.

We therefore add to our matrix element three additional diagrams with the two negative muons interchanged. The total set is depicted in Fig. 4. We square the complete set of diagrams, using the program SCHOONSCHIP and use this new trace in the computer program. The sign of the interference terms between the two sets is negative, causing a reduction in the size of the cross section and we divide the final answer by an additional factor of 2, to properly incorporate the Fermi-Dirac statistics for muons. As far as the event rate is concerned, we now find a small reduction in our answer of the order of 10%.

The numerical integration of the square of the whole matrix element is nontrivial because the propagators peak in different regions of phase space. It is difficult to get extremely accurate results without either lengthy computer runs on the full amplitude or a careful examination of the symmetry properties to reduce the number of terms. The matrix element for the set of graphs in Fig. 2 peaks dramatically in the variable $k^2 = (l_3 + l_4)^2$ which can easily be handled by a logarithmic mapping. The three additional diagrams in Fig. 4 have the same peaking in the variable $k'^2 = (l_2 + l_4)^2$ and yield the same value for the cross section. Hence it is difficult to follow both peaks. We avoid this problem by keeping the square of the first set and adding all the interference terms between the two sets with appropriate factors of 2. These terms can then be integrated by standard numerical methods. As we shall see in the next section the spectra for the two negative muons are significantly different which explains why the Pauli principle reduces the cross section by only 10%.

III. DISTRIBUTIONS

In this section we present our results for some of the distributions relevant for the experimental study of reaction (1). We only give these results after folding with the quadrupole-triplet spectrum and do not impose cuts on either the beam energy or the muon energies and angles. In the preceding section we discussed the consequences of including the Fermi-Dirac statistics for the muons, and found that this is a small effect which tends mainly to suppress the amplitude in the region where the muons have identical energies and angles. We ignore these complications here and follow the standard convention of binning the two negative muons according to their energy into fast and slow on an event-by-event basis. Hence we call E_1 the energy of the fast negatively charged muon, E_2 the energy of the slow negatively charged muon, and E_3 the energy of the positively charged muon.

In Fig. 5 we show the distributions in the energies of E_2 and E_3. The spectra are very similar although, owing to the rebinning, the average energy of E_2 is smaller than that of E_3. We also give the distribution in the energy of the slowest muon on an event-by-event basis. This distribution extends out to approximately 40 GeV and is useful for calculating the probability that the very energetic trimuon events seen by the FHPRW group can be accounted for by this process. In Fig. 6 we show the distributions in E_1 and in $E_{\rm had}$, the energy transferred to the hadrons. These distributions resemble their counterparts in the regular inclusive process $\nu_\mu + N \rightarrow \mu^- + X$. The average energies are calculated to be $\langle E_1 \rangle = 55$ GeV, $\langle E_2 \rangle = 14$ GeV,

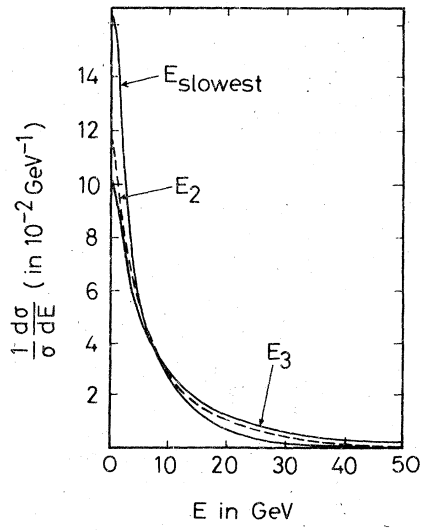

FIG. 5. The energy spectra for E_2, E_3, and $E_{\rm slowest}$ after folding with the quadrupole-triplet neutrino spectrum.

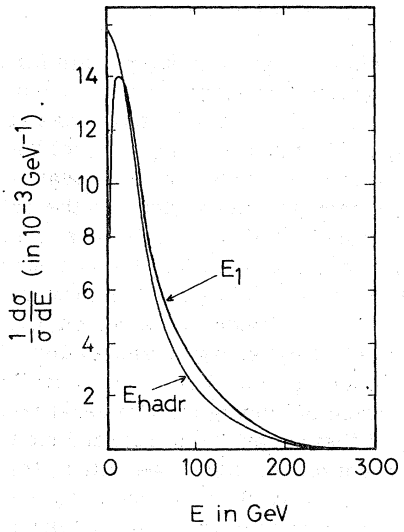

FIG. 6. The energy spectra for E_1 and E_{had}, after folding with the quadrupole-triplet neutrino spectrum.

$\langle E_3\rangle = 18$ GeV, and $\langle E_{had}\rangle = 60$ GeV.

We now give the distributions in the invariant masses, M_{123}, M_{12}, M_{13}, and M_{23} in Fig. 7. The trimuon invariant-mass spectrum is rather broad reflecting the fact that the radiation comes both from the muon and from the quarks. The distributions in M_{12} and M_{13} are also rather broad. However, the M_{23} spectrum is very sharply peaked at small masses reflecting the infrared tail of the photon spectrum. This last distribution is a key characteristic of the radiative process and any cut on M_{23} seriously reduces the signal from this electromagnetic reaction. We find that over 80% of the events have an M_{23} invariant mass less than

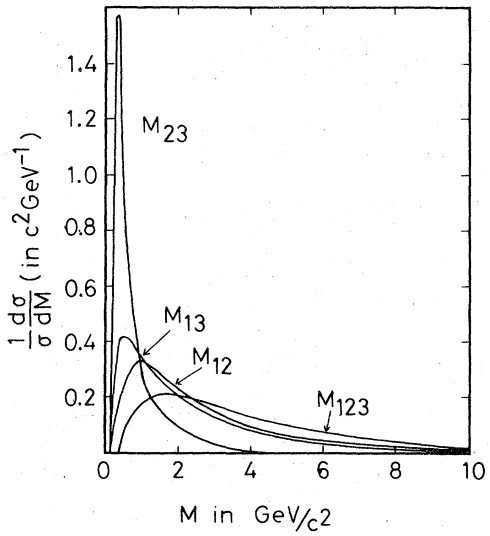

FIG. 7. The distributions in the invariant masses of the muons.

1 GeV/c^2. The average invariant masses are $\langle M_{123}\rangle = 3$ GeV/c^2, $\langle M_{12}\rangle = 2$ GeV/c^2, $\langle M_{13}\rangle = 1.9$ GeV/c^2, and $\langle M_{23}\rangle = 0.8$ GeV/c^2.

As far as the other distributions are concerned, there is nothing spectacular to report. The transverse momenta perpendicular to the direction of the neutrino beam are generally rather small, the largest being $p_{\perp,1}$. We find the averages to be $\langle p_{\perp,1}\rangle = 2.6$ GeV/c, $\langle p_{\perp,2}\rangle = 0.7$ GeV/c, and $\langle p_{\perp,3}\rangle = 0.8$ GeV/c. The visible energy distribution shows two distinctive peaks reflecting the presence of neutrinos from both pion and kaon decays. Since the threshold for the reaction is essentially zero, one expects a distribution in E_{vis} which is similar to the corresponding distribution in $\nu_\mu + N \to \mu^- + X$. There is a slightly larger peak for high-energy neutrinos due to the extra logarithms in the cross section. The average visible energy is 158 GeV.

We have also studied the opening angles between the muon transverse momenta vectors projected onto planes perpendicular to (1) the neutrino beam, (2) the W-boson direction defined with respect to the momentum of the fast μ^-, and (3) the plane perpendicular to the W-boson direction defined with respect to the sum of the momenta of the three muons. We have previously[4] called these planes the (x,y), (x',y'), and (x'',y'') planes, respectively, and will follow the same notation here. The corresponding angles we denote by ϕ, ϕ', and ϕ''. In the (x,y) plane it is interesting to see the distribution in the ϕ_{12} opening angle, because this distribution tells us the relative magnitudes of the radiation from the muon versus the radiation from the quarks. If there were no radiation at all, then the direction of the muon transverse momentum in the (x,y) plane is equal and opposite to the transverse momentum of the hadron shower. When the muon radiates then, on the average, the Dalitz pair tends to follow the direction of the muon. Similarly, when the radiation is from the hadrons (or quarks) then the Dalitz pair tends to follow the direction of the hadrons. Thus by examining ϕ_{12} and ϕ_{13} which are shown in Fig. 7, we see a forward peak from the radiation off the muon and a backward peak from the radiation off the hadrons. The ϕ_{23} distribution which is also seen in Fig. 7 does not show this feature. The average angles are $\langle\phi_{12}\rangle = 71°$, $\langle\phi_{13}\rangle = 65°$, and $\langle\phi_{23}\rangle = 57°$. When we project into the (x',y') plane, all the distributions begin to peak in the forward direction only. We give the distribution for ϕ'_{12} and ϕ'_{13} in Fig. 8. ϕ'_{23} peaks in much the same fashion but is not shown in Fig. 8. The averages now change to $\langle\phi'_{12}\rangle = 50°$, $\langle\phi_{13}\rangle = 42°$, and $\langle\phi_{23}\rangle = 46°$. The peaking increases even more in the (x'',y'') plane. We again show ϕ''_{12} and ϕ''_{13} in Fig. 8 but have neglected ϕ''_{23}. Our values for the averages now change to

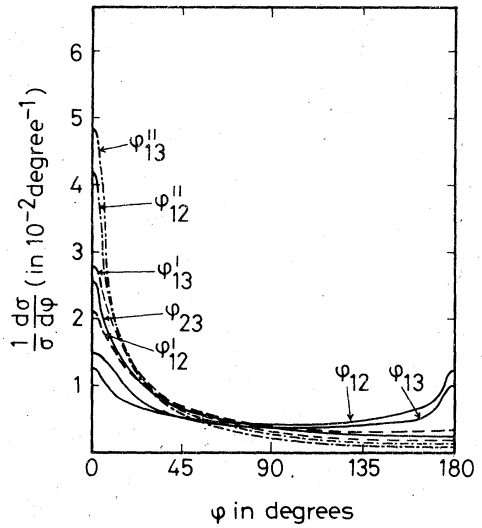

FIG. 8. The distributions in the ϕ angles between particular dimuon pairs.

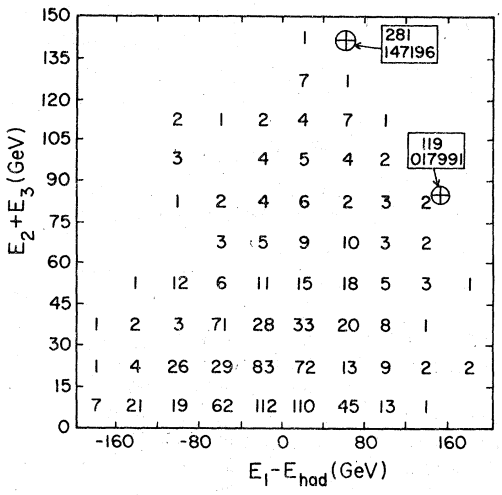

FIG. 9. Scatter plot of $E_1-E_{\rm had}$ versus E_2+E_3. The crosses represent the events 119 and 281 of the FHPRW group. The units are in GeV and the number of events is normalized to approximately 1000.

$\langle\phi''_{12}\rangle=33°$, $\langle\phi''_{13}\rangle=28°$, and $\langle\phi''_{23}\rangle=30°$.

For completeness we give the averages of the opening angles between the pairs of muons. We find $\langle\theta_{12}\rangle=0.13$ rad, $\langle\theta_{13}\rangle=0.10$ rad, and $\langle\theta_{23}\rangle=0.10$ rad. There are essentially no events with opening angles larger than 0.4 rad.

From the above results it is obvious that the electromagnetic process is important for low-invariant-mass dimuon pairs. There is also no energy lost into missing neutrinos, so it is important to ask whether the extremely energetic events seen by the FHPRW collaboration can possibly be explained by this mechanism. We have investigated this question in several ways, all of which lead to very low probabilities. We find in particular that a scatter plot of $E_{\rm had}$ versus the sum of the muon energies has very few events in the region around event numbers 119 and 281. Another correlation of the same type which is also helpful in distinguishing between different classes of models is to plot $E_1-E_{\rm had}$ versus E_2+E_3. We show the density of points in this latter plane in Fig. 9. The probability of events 119 and 281 being explained by Dalitz-pair production is approximately 0.1%. An examination of all the invariant masses of the pairs also shows that there is only a very low probability of accounting for these events.

IV. CONCLUSIONS

In this paper we have examined the production of $\mu^+\mu^-$ and e^+e^- Dalitz pairs in neutrino and antineutrino interactions. The rates for these processes are sufficiently large that their experimental detection should be relatively easy. In particular, for the reaction $\nu_\mu+N\to\mu^-+\mu^-+\mu^++X$, we find the event rate to be $\sim0.3\times10^{-4}$ of the normal inclusive reaction $\nu_\mu+N\to\mu^-+X$. This rate is large enough that some of the trimuon events already seen by the FHPRW and CDHS groups could be accounted for by this process. However, the extremely energetic events observed by the FHPRW group are unlikely to be candidates for the radiative reaction.

In Sec. III we have discussed several distributions which are characteristic of these processes. Essentially the radiation is a perturbation on the usual neutrino and antineutrino inclusive reaction, so the distributions for the fast μ^- and the hadrons are not changed significantly. The quantum-electrodynamical character of the radiation manifests itself in the extreme peaking of the invariant mass of the slow μ^- and the μ^+. The other invariant mass distributions are not peaked in any dramatic fashion, in particular the M_{123} distribution is rather broad. In the reactions where e^+e^- pairs are emitted, there is no ambiguity about the origin of the negatively charged particles, and the e^+e^- invariant mass peaks even more sharply at small masses. Our examination of the inclusion of Fermi-Dirac statistics for muons shows that the Pauli exclusion principle does not product significant changes in our results.

We have limited our discussion here to multimuon production in a wide band beam. Obviously the estimates of the event rates will change slightly if narrow band beams are employed. In general, our results will decrease in that situation because the extra logarithmic factors in the beam energy are less important.

To conclude we would like to reiterate that the experimental study of these reactions will provide us with useful information and allow a test of the quark-parton model.

ACKNOWLEDGMENTS

We would like to acknowledge useful conversations with Professor A. Mann concerning the present status of the FHPRW data. We have also discussed technical aspects of this calculation with M. Barnett, N. Weiss, T. Gottschalk, and V. Barger. Some of this work was carried out at Fermilab and we would like to thank C. Quigg for hospitality. This work was supported in part by the National Science Foundation under Grant No. PHY-76-15328 and by the Department of Energy.

[1]B. C. Barish *et al.*, Phys. Rev. Lett. 38, 577 (1977).
[2]A. Benvenuti *et al.*, Phys. Rev. Lett. 38, 1110 (1977); A. Benvenuti *et al.*, *ibid.* 40, 488 (1978).
[3]M. Holder *et al.*, Phys. Lett. 70B, 393 (1977).
[4]A. Benvenuti *et al.*, Phys. Rev. Lett. 38, 1183 (1977); C. H. Albright, J. Smith, and J. A. M. Vermaseren, *ibid.* 38, 1187 (1977); Phys. Rev. D 16, 3182 (1977); 16, 3204 (1977); V. Barger, T. Gottschalk, D. V. Nanopoulos, J. Abad, and R. J. N. Phillips, Phys. Rev. Lett. 38, 1190 (1977); Phys. Rev. D 16, 2141 (1977); 16, 3170 (1977); 16, 3177 (1977); see also University of Wisconsin Report No. COO-597 (unpublished); Phys. Lett. 70B, 243 (1977); P. Langacker and G. Segrè, Phys. Rev. Lett. 39, 259 (1977); P. Langacker, G. Segrè, and M. Golshani, Phys. Rev. D 17, 1402 (1978); B. W. Lee and S. Weinberg, Phys. Rev. Lett. 38, 1239 (1977); B. W. Lee and R. E. Shrock, Phys. Rev. D 17, 2410 (1978), C. H. Albright, R. E. Schrock, and J. Smith, Phys. Rev. D 17, 2383 (1978); R. M. Barnett and L.-N. Chang, Phys. Lett. 72B, 233 (1977); R. M. Barnett, L. N. Chang, and N. Weiss, Phys. Rev. D 17, 2266 (1978); A. Soni, Phys. Lett. 71B, 435 (1977).
[5]F. Bletzacker, H. T. Nieh, and A. Soni, Phys. Rev. Lett. 38, 1241 (1977); F. Bletzacker and H. T. Nieh, Stony Brook Report No. ITP-SB-77-42 (unpublished).
[6]R. Godbole, Phys. Rev. D (to be published).
[7]J. J. Russell *et al.*, Phys. Rev. Lett. 26, 46 (1971).
[8]C. Chang, K. W. Chen, and A. van Ginneken, Phys. Rev. Lett. 39, 519 (1977).
[9]F. Bletzacker and H. T. Nieh, Stony Brook Report No. ITP-SB-77-44 (unpublished).
[10]D. L. Fancher *et al.*, Phys. Rev. Lett. 38, 800 (1977).
[11]J. F. Davis *et al.*, Phys. Rev. Lett. 29, 1356 (1972).
[12]D. O. Caldwell *et al.*, Phys. Rev. Lett. 33, 868 (1974).
[13]J. Kiskis, Phys. Rev. D 8, 2129 (1973).
[14]R. W. Brown, R. H. Hobbs, J. Smith, and N. Stanko, Phys. Rev. D 6, 3273 (1972); K. Fujikawa, Ann. Phys. (N.Y.) 68, 102 (1971); 75, 491 (1973).
[15] SCHOONSCHIP is an algebraic program written by M. Veltman. See H. Strubbe, Comput. Phys. Commun. 8, 1 (1974).
[16]J. Okada, S. Pakvasa, and S. F. Tuan, Lett. Nuovo Cimento 16, 555 (1976). For an alternative parametrization of the structure functions see R. D. Field and R. P. Feynman, Phys. Rev. D 15, 2590 (1977).
[17]The exponent in the sea distribution is now known to be larger than 3.5 [M. Holder *et al.*, Phys. Lett. 69B, 377 (1977)]. We have increased the size of the exponent to 7 but it makes no changes in our results. We thank Professor Kleinknecht for bringing this point to our attention.